Physics Letters B 781 (2018) 553–560

Contents lists available at ScienceDirect

Physics Letters B

www.elsevier.com/locate/physletb

Thermal fluctuations of dilaton black holes in gravity's rainbow

M. Dehghani

Department of Physics, Razi University, Kermanshah, Iran

ARTICLE INFO

Article history:
Received 31 March 2018
Received in revised form 19 April 2018
Accepted 19 April 2018
Available online 24 April 2018
Editor: N. Lambert

Keywords:
Four-dimensional black hole
Black hole with scalar hair
Rainbow gravity
Thermal fluctuations

ABSTRACT

In this work, thermodynamics and phase transition of some new dilaton black hole solutions have been explored in the presence of the rainbow functions. By introducing an energy dependent space time, the dilaton potential has been obtained as the linear combination of two Liouville-type potentials and three new classes of black hole solutions have been constructed. The conserved and thermodynamic quantities of the new dilaton black holes have been calculated in the energy dependent space times. It has been shown that, even if some of the thermodynamic quantities are affected by the rainbow functions, the thermodynamical first law still remains valid. Also, the impacts of rainbow functions on the stability or phase transition of the new black hole solutions have been investigated. Finally, the quantum gravitational effects on the thermodynamics and phase transition of the solutions have been studied through consideration of the thermal fluctuations.

1. Introduction

Promoting of the usual energy-momentum dispersion relation to the modified dispersion relation is one of the findings of loop quantum gravity and the quantum models based on the non-commutative geometry [1–6]. This modification which is realized at the Planck-scale regime leads to the violation of the Lorentz symmetry as one of the most important symmetries in the universe. The deformed or doubly special relativity, as a modified formalism of special relativity, has been proposed to preserve Lorentz symmetry in the modified dispersion relation [6–8]. In the high energy formalism of the special relativity, known as the doubly special relativity, in addition to the speed of light the Planck energy is considered as a universal constant. In this theory, it is impossible for a particle to attain an energy and a velocity greater than the Planck energy and light velocity, respectively. It is accomplished by utilizing a nonlinear Lorentz transformation in the momentum space in a way that the energy-momentum relation appears with the corrections in the order of the Planck length. Also the Planck-scale corrected dispersion relation preserves a deformed Lorentz symmetry [9–11]. It seems that the violation of Lorentz symmetry plays an essential rule in constructing the quantum theory of gravity. It is notable that, due to the existence of an unstable perturbative string vacuum, violation of the Lorentz symmetry can also occur in the string theory [12].

Recently, Magueijo and Smolin have extended the doubly special relativity to the curved space times. This doubly general theory of relativity is called rainbow gravity (or gravity's rainbow) [13]. The name rainbow gravity comes from the fact that in this theory the space time geometry depends on the energy of a test particle E. Therefore, instead of a single metric, there is a family of metrics (rainbow metrics) which are parameterized by the ratio $\varepsilon = E/E_p$, where E_P denotes the Planck energy [14]. Therefore, gravity's rainbow, just like the Horava–Lifshitz gravity theory, can be considered as the ultraviolet completion of the Einstein's general relativity. There is a close relation between the rainbow and Horava–Lifshitz gravity theories. Both of them are based on promoting of the usual dispersion relation to the modified dispersion relation [15–17]. As pointed out by many authors, a general modified dispersion relation may be written as [18–23]

$$E^2 f^2(\varepsilon) - p^2 g^2(\varepsilon) = m^2, \tag{1.1}$$

where, the functions $f(\varepsilon)$ and $g(\varepsilon)$ are known as the rainbow functions, which are required to satisfy the following conditions

$$\lim_{\varepsilon\to 0} f(\varepsilon) = 1, \quad \text{and} \quad \lim_{\varepsilon\to 0} g(\varepsilon) = 1. \tag{1.2}$$

By these requirements the standard dispersion relation can be recovered in the infrared limit of the theory. It must be noted that different functional forms of the rainbow functions are proposed which are based on different phenomenological motivations. Some of the proposed models for the temporal and spatial rainbow functions can be found in Refs. [24–28].

E-mail address: m.dehghani@razi.ac.ir.

https://doi.org/10.1016/j.physletb.2018.04.039

In this work, motivated by the new and interesting findings of gravity's rainbow such as black hole remnant [29,30] and nonsingular universe [31], we are interested in investigating of thermodynamic properties of dilatonic black hole solutions in gravity's rainbow. After the discoveries of Hawking et al., the black holes are considered as thermodynamic systems with well-defined thermodynamic properties such as entropy and temperature [32–36]. Although, the black hole thermodynamics is an important issue and has been studied extensively, it still has many interesting parts to be studied [37–42]. Study of the quantum gravitational effects on the black hole thermodynamics is a more attractive subject (see Refs. [43–47] for example). In addition, it is commonly believed that black holes are examples of extreme quantum gravity regimes and for a complete description the quantum gravitational effects cannot be forgotten. Also, through consideration of the black hole thermal fluctuations, we tend to investigate the quantum gravitational effects on the thermodynamic properties and thermal stability of dilaton black holes in the presence of rainbow functions. It has been demonstrated that the black hole thermal fluctuations are corresponded to the quantum fluctuations on the space time geometry [48]. The impacts of quantum gravity theory, via consideration of the thermal fluctuations, have been studied by Pourhassan et al. for a variety of black holes [49–53]. Also, this issue has been studied by Hendi et al. for the Einstein–Born–Infeld black holes in rainbow gravity [18].

The paper is outlined as follows: In section 2, by introducing a spherically symmetric and energy dependent geometry, the coupled field equations of the scalar and gravitational field equations have been solved. The dilatonic potential has been calculated and it has been written as the linear combination of two exponential potentials known as the Liouville-type potentials. Three new classes of dilatonic black hole solutions have been obtained as the exact solutions to the gravitational field equations. It has been shown that the asymptotic behavior of the solutions is neither flat nor A(dS). Section 3 is devoted to the study of thermodynamic properties of the dilaton black holes, obtained here. The temperature and entropy of the black holes have been calculated based on the concept of the surface gravity and the entropy-area law, respectively. Through a Smarr-type mass formula, the black hole mass has been written as a function of the black hole entropy. It has been found that, even in the presence of the rainbow functions, the first law of black hole thermodynamics remains valid. A black hole thermal stability or phase transition analysis has been performed based on the canonical ensemble method and regarding the signature of the black hole heat capacity. The points of type-1 and type-2 phase transitions as well as the ranges at which the physical black holes remain stable are determined, exactly. In section 4, in order to investigate the quantum gravitational effects on the thermodynamic phase transition of the black holes, the thermal fluctuations of the solutions have been studied. The quantum corrected thermodynamic quantities have been calculated and validity of the first law of black hole thermodynamics has been confirmed. By calculating the quantum corrected black hole heat capacity the impacts of thermal fluctuations on the black hole stability have been studied. Some concluding remarks and discussions are summarized in section 5.

2. The black hole solutions in the energy dependent space times

The suitable Lagrangian of the four-dimensional Einstein-dilaton gravity theory can be written in the following general form [40,41], [54–56]

$$\mathcal{L} = \mathcal{R} - V(\phi) - 2(\nabla\phi)^2. \tag{2.1}$$

Here, $\mathcal{R}$ is the Ricci scalar, ϕ is a scalar field coupled to itself via the functional form $V(\phi)$. By varying the action (2.1) with respect to the gravitational and scalar fields, we get the following field equations

$$\mathcal{R}_{\mu\nu} - \frac{1}{2}g_{\mu\nu}V(\phi) - 2\nabla_\mu\phi\nabla_\nu\phi = 0, \tag{2.2}$$

$$4\Box\phi = \frac{dV(\phi)}{d\phi}, \qquad \phi = \phi(r). \tag{2.3}$$

We would like to solve these field equations in a four-dimensional spherically symmetric geometry with the following line element [18–20]

$$ds^2 = -\frac{N(r)}{f^2(\varepsilon)}dt^2 + \frac{1}{g^2(\varepsilon)N(r)}dr^2 + \frac{r^2R^2(r)}{g^2(\varepsilon)}(d\theta^2 + \sin^2\theta d\varphi^2). \tag{2.4}$$

In order to obtain the metric function $N(r)$, we use Eq. (2.4) in the gravitational field equations (2.2). It leads to the following differential equations

$$e_{tt} = N''(r) + 2\left(\frac{1}{r} + \frac{R'(r)}{R(r)}\right)N'(r) + \frac{V(\phi)}{g^2(\varepsilon)} = 0, \tag{2.5}$$

$$e_{rr} = e_{tt} + 4g^2(\varepsilon)\left(\frac{R''(r)}{R(r)} + \frac{2R'(r)}{rR(r)} + (\phi'(r))^2\right)N(r) = 0, \tag{2.6}$$

$$e_{\theta\theta} = e_{\varphi\varphi} = \left(\frac{1}{r^2} + \frac{R''(r)}{R(r)} + \frac{4R'(r)}{rR(r)} + \frac{R'^2(r)}{R^2(r)}\right)N(r) + \left(\frac{1}{r} + \frac{R'(r)}{R(r)}\right)N'(r) - \frac{1}{r^2R^2(r)} + \frac{V(\phi)}{2g^2(\varepsilon)} = 0, \tag{2.7}$$

for the tt, rr and $\theta\theta$ ($\varphi\varphi$) components, respectively. Regarding Eqs. (2.5) and (2.6) we have

$$\frac{R''(r)}{R(r)} + \frac{2}{r}\frac{R'(r)}{R(r)} + \phi'^2(r) = 0, \tag{2.8}$$

which can be rewritten in the following form

$$\frac{2}{r}\frac{d}{dr}\ln R(r) + \frac{d^2}{dr^2}\ln R(r) + \left(\frac{d}{dr}\ln R(r)\right)^2 + 2(\phi'(r))^2 = 0. \tag{2.9}$$

It is understood from Eq. (2.9) that $R(r)$ can be written as an exponential function of $\phi(r)$. Thus, we can use exponential solutions of the form $R(r) = e^{\alpha\phi}$ in Eq. (2.8). One can show that $\phi = \phi(r)$ satisfies the following differential equation

$$\alpha\phi'' + (1 + 2\alpha^2)\phi'^2 + \frac{2\alpha}{r}\phi' = 0. \tag{2.10}$$

The solution to the differential equation (2.10), in terms of a positive constant b, can be written as

$$\phi(r) = \gamma\ln\left(\frac{b}{r}\right), \quad \text{with} \quad \gamma = \alpha(1 + \alpha^2)^{-1}. \tag{2.11}$$

It must be mentioned that, a similar solution has been used previously for charged and uncharged dilaton black hole solutions [40,41,54].

Now, making use of these solutions in Eqs. (2.3) and (2.7), after some algebraic calculations, we have

$$\frac{1 - \alpha\gamma}{r}\left(N' + \frac{1 - 2\alpha\gamma}{r}N\right) - \frac{1}{r^2R^2} + \frac{V(\phi)}{2g^2(\varepsilon)} = 0, \tag{2.12}$$

$$\frac{dV(\phi)}{d\phi}-\frac{2\gamma}{1-\alpha\gamma}V(\phi)+\frac{4g^2(\varepsilon)\gamma}{1-\alpha\gamma}\frac{1}{r^2R^2}=0. \tag{2.13}$$

In terms of an integration constant C, the solution of Eq. (2.13), can be obtained as

$$V(\phi)=\frac{-2\alpha^2g^2(\varepsilon)}{b^2(1-\alpha^2)}e^{2\left(\frac{1}{\gamma}-\alpha\right)\phi}+Ce^{\frac{2\gamma}{1-\alpha\gamma}\phi}. \tag{2.14}$$

Noting the fact that, in the absence of the dilaton field (i.e. $\phi=0$ or equivalently $\alpha=0=\gamma$) the Lagrangian (2.1) reduces to that of Einstein gravity with cosmological constant, one can obtain the constant C by imposing the condition $V(\phi=0)=2\Lambda$. It results in $C=2\Lambda=-6\ell^{-2}$.

Now, the complete solution to Eq. (2.13) can be written in the following form

$$V(\phi)=\begin{cases}2\Lambda e^{2\theta\phi}+2\Lambda_1e^{2\theta_1\phi}, & \alpha\neq 1,\\ 2\Lambda e^{2\phi}+2\lambda_1\phi e^{2\phi}, & \alpha=1,\end{cases} \tag{2.15}$$

where

$$\Lambda_1=\frac{-\alpha^2g^2(\varepsilon)}{b^2(1-\alpha^2)},\quad \theta=\frac{\gamma}{1-\alpha\gamma}=\frac{1}{\theta_1},\quad \lambda_1=-\frac{2g^2(\varepsilon)}{b^2}.$$

Eq. (2.15) shows that the dilatonic potential can be written as the linear combination of two Liouville-type potentials.

Making use of Eqs. (2.12) and (2.15), after some manipulations, we obtained the metric function $N(r)$ as

$$N(r)=\begin{cases}\frac{-m}{r^{1-2\alpha\gamma}}+\frac{1+\alpha^2}{1-\alpha^2}\left[\left(\frac{b}{r}\right)^{-2\alpha\gamma}\right.\\ \quad\left.+\frac{3b^2(1-\alpha^4)}{g^2(\varepsilon)\ell^2(3-\alpha^2)}\left(\frac{b}{r}\right)^{2(\alpha\gamma-1)}\right], \quad \alpha\neq 1,\ \sqrt{3},\quad (a)\\ -mr^{\frac{1}{2}}-2\left(\frac{b}{r}\right)^{-\frac{3}{2}}\left[1-\frac{6b^2}{g^2(\varepsilon)\ell^2}\left(\frac{b}{r}\right)\ln\left(\frac{r}{b}\right)\right],\\ \quad\alpha=\sqrt{3},\quad (b)\\ -m+2\left[2-\frac{\Lambda b^2}{g^2(\varepsilon)}\right.\\ \quad\left.+\ln\left(\frac{b}{r}\right)\right]\left(\frac{r}{b}\right), \quad \alpha=1,\ (c)\end{cases} \tag{2.16}$$

where, m is an integration constant related to the black hole mass. It is notable that in the absence of the dilatonic field (i.e. $\alpha=0=\gamma$), if we set $g^2(\varepsilon)=1$ the metric function $N(r)$ reduces to the metric function of Schwarzschild-A(dS) black holes.

In order to investigate the existence and the number of real roots of the metric function $N(r)$, it is better to use the plots of $N(r)$ versus r. Thus we need to have the numerical values of $f(\varepsilon)$ and $g(\varepsilon)$. The explicit forms of these functions can be written as [24–28]

$$f(\varepsilon)=1,\quad \text{and}\quad g(\varepsilon)=\sqrt{1-\eta\varepsilon^n}, \tag{2.17}$$

$$f(\varepsilon)=\frac{e^{\zeta\varepsilon}-1}{\zeta\varepsilon},\quad \text{and}\quad g(\varepsilon)=1, \tag{2.18}$$

$$f(\varepsilon)=g(\varepsilon)=\frac{1}{1-\beta\varepsilon}. \tag{2.19}$$

The coefficients η, ζ and β, known as the rainbow parameters, are of the order of unity, $\varepsilon\leq 1$ and the power n is a positive integer [23,29,31]. Therefore, the numerical values of the temporal and spatial rainbow functions can be approximated as equal to or slightly less or more than unity. We choose the numerical values of $f(\varepsilon)$ and $g(\varepsilon)$ similar to those have been used in Refs. [18,19]. This covers almost all of the proposed functional forms of the rainbow functions.

The plots of $N(r)$ versus r are shown in Figs. 1–3 for the cases $\alpha\neq 1$, $\sqrt{3}$, $\alpha=\sqrt{3}$ and $\alpha=1$, respectively. The impacts of dilaton parameter α and the rainbow functions $f(\varepsilon)$ and $g(\varepsilon)$ have been considered in the Figs. 1–3. A notable point is that, they can show the two horizon, extreme and naked singularity dilaton black holes for the properly fixed parameters.

The curvature singularities of the black hole solutions can be considered through the Ricci and Kretschmann scalars. It is a matter of calculation to show that the Ricci and Kretschmann scalars are finite for finite values of the radial component r. Also, we have

$$\lim_{r\longrightarrow\infty}\mathcal{R}=0,\qquad \text{and}\qquad \lim_{r\longrightarrow 0}\mathcal{R}=\infty, \tag{2.20}$$

$$\lim_{r\longrightarrow\infty}\mathcal{R}^{\mu\nu\rho\lambda}\mathcal{R}_{\mu\nu\rho\lambda}=0,\quad \text{and}$$
$$\lim_{r\longrightarrow 0}\mathcal{R}^{\mu\nu\rho\lambda}\mathcal{R}_{\mu\nu\rho\lambda}=\infty. \tag{2.21}$$

Therefore, there is an essential (not coordinate) singularity located at the origin which can be interpreted as the existence of the black hole solutions. Also, in the presence of dilaton fields, the asymptotic behavior of the solutions are neither flat nor A(dS).

3. Thermodynamics

This section is devoted to calculation of the conserved and thermodynamic quantities related to the new dilaton black hole solutions obtained here. For this purpose we use the geometrical and the thermodynamical approaches. Then, with the help of the obtained thermodynamic quantities, we investigate the validity of the first law of black hole thermodynamics. At first, making use of the concept of the black hole surface gravity κ, we calculate the Hawking temperature associated to the black hole horizon. That is

$$T=\frac{\kappa}{2\pi}=\frac{1}{4\pi r_+}\frac{g(\varepsilon)}{f(\varepsilon)}$$
$$\times\begin{cases}\frac{1+\alpha^2}{1-\alpha^2}\left(\frac{b}{r_+}\right)^{-2\alpha\gamma}\left[1+\frac{3b^2(1-\alpha^2)}{g^2(\varepsilon)\ell^2}\left(\frac{b}{r_+}\right)^{2(2\alpha\gamma-1)}\right],\\ \quad\alpha\neq\sqrt{3},\ 1,\ (a)\\ 2\left(\frac{r_+}{b}\right)^{\frac{1}{2}}\left(\frac{6b^2}{g^2(\varepsilon)\ell^2}-\frac{r_+}{b}\right), \quad \alpha=\sqrt{3},\quad (b)\\ \frac{2r_+}{b}\left[1-\frac{\Lambda b^2}{g^2(\varepsilon)}+\ln\left(\frac{b}{r_+}\right)\right], \quad \alpha=1.\ (c)\end{cases} \tag{3.1}$$

It must be noted that we have used the relation $N(r_+)=0$ for eliminating the mass parameter, m, from the above relations. The temperature of the black holes corresponding to $\alpha\neq\sqrt{3},1$ is positive valued for $\alpha^2<1$ (Fig. 4). Also, the extreme black holes (i.e. the black holes with zero temperature) may occur for $\alpha^2>1$ provided that the black hole horizon radius, $r_+=r_{ext}$, satisfies the following relation

$$r_{ext}=b\left(\frac{3b^2(\alpha^2-1)}{g^2(\varepsilon)\ell^2}\right)^{\frac{\alpha^2+1}{2(\alpha^2-1)}},\quad \alpha\neq\sqrt{3},\ 1, \tag{3.2}$$

and the physical black holes, having positive temperature, occur if $r_+<r_{ext}$. The un-physical black holes (i.e. the black holes with negative temperature) are those with the horizon radius greater than r_{ext}.

In the case $\alpha=\sqrt{3}$, the extreme black holes have a horizon radius given by the following equation

$$r_{3ext}=\frac{6b^3}{g^2(\varepsilon)\ell^2},\qquad \alpha=\sqrt{3}, \tag{3.3}$$

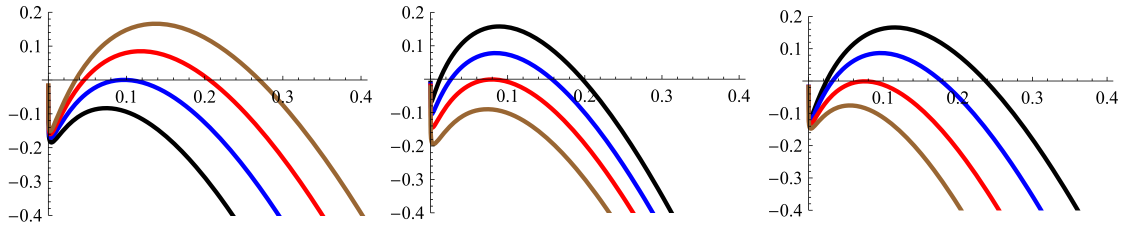

Fig. 1. $N(r)$ versus r for $b = 0.5$, $M = 0.2$, $\ell = 1$ and $\alpha \neq 1, \sqrt{3}$, Eq. (2.16-a). Left: $f(\varepsilon) = 0.38$, $g(\varepsilon) = 0.85$ and $\alpha = 1.215, 1.2247, 1.233, 1.24$ for black, blue, red and brown curves, respectively. Middle: $\alpha = 1.2$, $g(\varepsilon) = 0.8$ and $f(\varepsilon) = 0.18, 0.25, 0.32, 0.4$ for black, blue, red and brown curves, respectively. Right: $\alpha = 1.2$, $f(\varepsilon) = 0.3$ and $g(\varepsilon) = 0.76, 0.78, 0.808, 0.84$ for black, blue, red and brown curves, respectively. (For interpretation of the colors in the figure(s), the reader is referred to the web version of this article.)

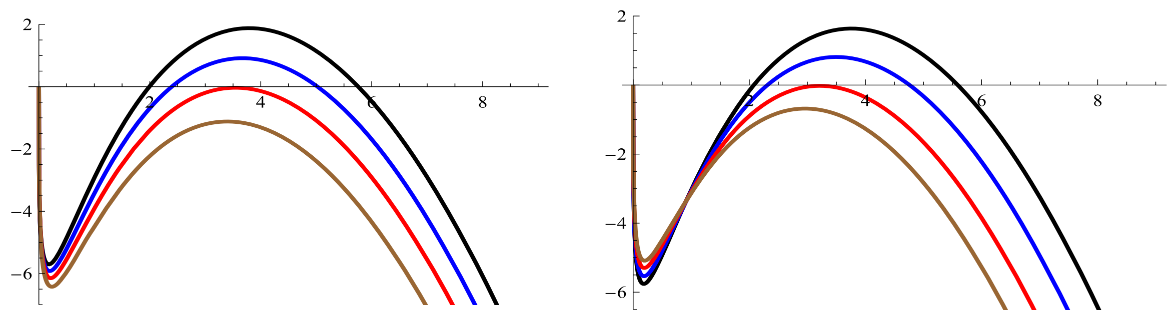

Fig. 2. $N(r)$ versus r for $\ell = 1$, $M = 0.4$, $b = 1$ and $\alpha = \sqrt{3}$, Eq. (2.16-b). Left: $g(\varepsilon) = 1.3$ and $f(\varepsilon) = 0.22, 0.34, 0.46, 0.6$ for black, blue, red and brown curves, respectively. Right: $f(\varepsilon) = 0.25$ and $g(\varepsilon) = 1.3, 1.33, 1.66, 1.4$ for black, blue, red and brown curves, respectively.

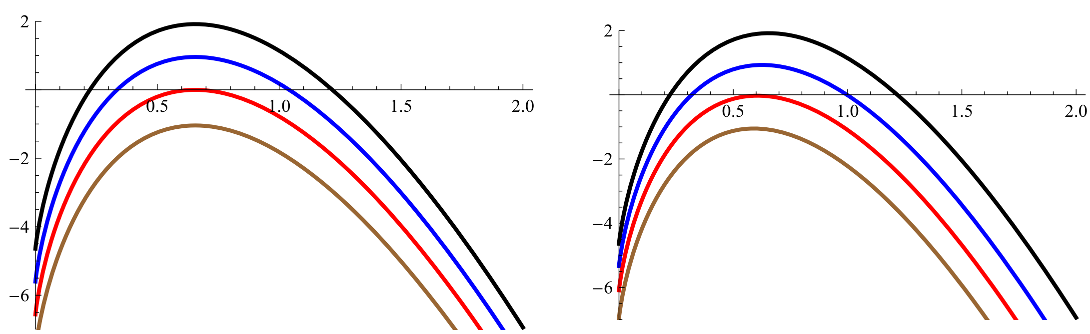

Fig. 3. $N(r)$ versus r for $\Lambda = -3$, $M = 0.5$, $b = 0.2$ and $\alpha = 1$, Eq. (2.16-c). Left: $g(\varepsilon) = 0.8$ and $f(\varepsilon) = 0.58, 0.7, 0.82, 0.95$ for black, blue, red and brown curves, respectively. Right: $f(\varepsilon) = 0.58$ and $g(\varepsilon) = 0.8, 0.92, 1.05, 1.2$ for black, blue, red and brown curves, respectively.

and the physical and un-physical black holes occur for $r_+ < r_{3ext}$ and $r_+ > r_{3ext}$, respectively.

It is easily shown that the horizon radius for the extreme black holes in the case $\alpha = 1$ is located at

$$r_{1ext} = be^{1-\frac{\Lambda b^2}{g^2(\varepsilon)}}, \qquad \alpha = 1. \tag{3.4}$$

They are physically reasonable if $r_+ < r_{1ext}$, otherwise they are not physically acceptable because of their negative temperatures.

Next, the black hole entropy, as a pure geometrical quantity, can be obtained making use of the Hawking–Bekenstein entropy-area law. According to the Hawking–Bekenstein entropy-area law, black hole entropy is equal to one-fourth of the black hole horizon area. Thus, making use of this nearly universal law, we can write

$$S = \frac{A}{4} = \pi r_+^2 \left(R(r_+)\right)^2 = \pi r_+^2 \left(\frac{b}{r_+}\right)^{2\alpha\gamma}, \tag{3.5}$$

which reduces to that of Schwarzschild-A(dS) black holes when the dilatonic field disappears.

The conserved mass of the black hole can be obtained in terms of the mass parameter m. It is a matter of calculation to show that the total mass of the new dilatonic black holes in rainbow gravity can be obtained as [18,19,54]

$$m = 2Mf(\varepsilon)g(\varepsilon)(1+\alpha^2)b^{-2\alpha\gamma}. \tag{3.6}$$

Note that in the infrared limit (i.e. $f(\varepsilon) = 1$ and $f(\varepsilon) = 1$), Eq. (3.6) is compatible with the mass of dilaton black holes [55] and by setting $\alpha = 0 = \gamma$ it coincides with the mass of the Schwarzschild-A(dS) black holes.

Making use of the fact that the black hole horizon radiuses are the real roots of the relation $N(r_+) = 0$ and by combining the result with Eqs. (3.5) and (3.6), one can obtain the black hole mass as a function of the black hole entropy (the only thermodynamical extensive parameter). After some simple calculations, we arrived at the following Smarr-type mass formula

$$M(S)=\begin{cases}\frac{b}{2f(\varepsilon)g(\varepsilon)(1-\alpha^2)}\left[\frac{r_+(S)}{b}\right.\\ \quad\left.+\frac{3b^2(1-\alpha^4)}{g^2(\varepsilon)\ell^2(3-\alpha^2)}\left(\frac{b}{r_+(S)}\right)^{4\alpha\gamma-3}\right], & \alpha\neq 1,\ \sqrt{3},\\ \frac{b}{4f(\varepsilon)g(\varepsilon)}\left[\frac{6b^2}{g^2(\varepsilon)\ell^2}\ln\left(\frac{r_+(S)}{b}\right)\right.\\ \quad\left.-\frac{r_+(S)}{b}\right], & \alpha=\sqrt{3},\\ \frac{b}{2f(\varepsilon)g(\varepsilon)}\left[2-\frac{\Lambda b^2}{g^2(\varepsilon)}\right.\\ \quad\left.+\ln\left(\frac{b}{r_+(S)}\right)\right]\left(\frac{r_+(S)}{b}\right), & \alpha=1.\end{cases} \tag{3.7}$$

Now, making use of Eqs. (3.5) and (3.7), it is easily shown that

$$\left(\frac{\partial M}{\partial S}\right)_Q=\left(\frac{\partial M}{\partial r_+}\right)_Q\left(\frac{\partial S}{\partial r_+}\right)_Q^{-1}=T. \tag{3.8}$$

Therefore, we proved that the first law of black hole thermodynamics is valid, for all of the three new dilatonic black hole solutions, in the following form

$$dM=TdS. \tag{3.9}$$

Now, we are in the position to investigate the thermal stability or phase transition of the new dilaton black hole solutions, obtained here. In order to perform a thermal stability analysis we need to calculate the black hole heat capacity. It is given by the relation [56,57]

$$C=T\frac{\partial S}{\partial T}. \tag{3.10}$$

From the view point of the canonical ensemble method, the positivity of the black hole heat capacity is sufficient to ensure the thermal stability of the physical black holes. Unstable black holes undergo phase transition to be stabilized. The points at which the black hole heat capacity vanishes are known as the points of type-1 phase transition. The divergent points of the black hole heat capacity are the points where the type-2 phase transition takes place [58–60]. With these issues in mind and making use of Eq. (3.10), we proceed to perform a stability analysis regarding the signature of the black hole heat capacity. It is a matter of calculation to show that the black hole heat capacity can be written in the following form

$$C=\begin{cases}\frac{2\pi b(\Upsilon-1)}{g^2(\varepsilon)(1-\alpha^2)(\Upsilon+1)}\left(\frac{b}{r_+}\right)^{2\alpha\gamma}, & \alpha\neq 1,\ \sqrt{3},\ (a)\\ \frac{\pi b^2(1+\Upsilon_3)}{g^2(\varepsilon)(1-\Upsilon_3)}\left(\frac{r_+}{b}\right)^{\frac{1}{2}}, & \alpha=\sqrt{3}, \quad (b)\\ -\frac{b\Lambda r_+}{g^2(\varepsilon)}\left[1-\frac{\Lambda b^2}{g^2(\varepsilon)}+\ln\left(\frac{b}{r_+}\right)\right], & \alpha=1, \quad (c)\end{cases} \tag{3.11}$$

where

$$\Upsilon=\frac{\Lambda b^2}{g^2(\varepsilon)}(1-\alpha^2)\left(\frac{b}{r_+}\right)^{2(2\alpha\gamma-1)}, \text{ and } \Upsilon_3=\frac{2\Lambda b^3}{g^2(\varepsilon)r_+}. \tag{3.12}$$

In order to find the points of type-1 and type-2 phase transitions as well as the ranges at which the black holes are locally stable, we have plotted the black hole heat capacity versus r_+ in Figs. 4 and 5.

It is clear from Fig. 4 that, for the properly chosen parameters, the black holes with a positive valued temperature do not undergo type-1 phase transition. There is point of type-2 phase transition located at $r_+=r_0$, where the black hole heat capacity diverges. The heat capacity is positive for $r_+>r_0$ and the physical black holes with the horizon radius in this range are locally stable. The left and right panels of Fig. 5 show the temperature and heat capacity of the black holes with $\alpha=\sqrt{3}$ and $\alpha=1$, respectively. There is a point of type-1 phase transition located at $r_+=r_{3ext}$ and $r_+=r_{1ext}$ in order for $\alpha=\sqrt{3}$ and $\alpha=1$ cases. No type-2 phase transition occurs for these kinds of black hole solutions. The physical black holes (i.e. black holes with positive temperature) are unstable. A notable point is that the points of type-1 phase transition coincide with the horizon radius of the extreme black holes.

4. The corrections from thermal fluctuations

Now, we investigate the impacts of thermal fluctuations on the thermodynamic stability of our new dilaton black holes. Thus, we need to calculate the modified thermodynamic quantities in the presence of thermal fluctuations. Regarding the concept of surface

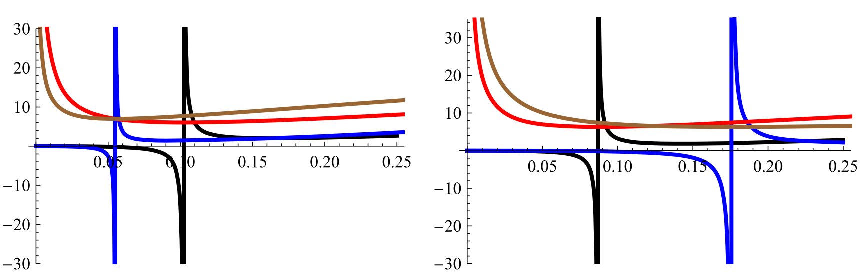

Fig. 4. T and C versus r_+ for $\Lambda=-3$, $f(\varepsilon)=0.5$ and $b=2.5$, Eqs. (3.1-a) and (3.11-a). Left: $g(\varepsilon)=0.25$, [$10\,T$: $\alpha=0.25, 0.4$, for red and brown curves, respectively] and [$0.2C$: $\alpha=0.25, 0.4$, for black and blue curves, respectively]. Right: $\alpha=0.3$, [$10\,T$: $g(\varepsilon)=0.25, 0.45$, for red and brown curves, respectively] and [$0.2C$: $g(\varepsilon)=0.25, 0.45$, for black and blue curves, respectively].

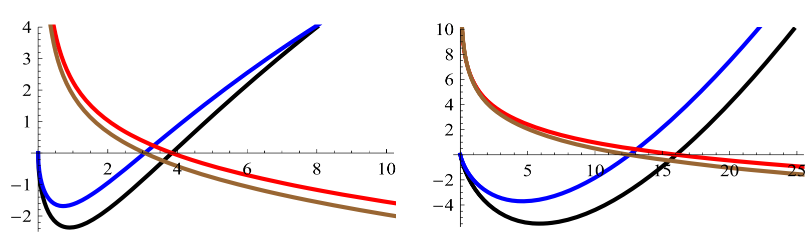

Fig. 5. T and C versus r_+ for $\Lambda=-3$, $f=0.5$ and $b=1$, Eqs. (3.1-b,c) and (3.11-b,c). Left: $\alpha=\sqrt{3}$ [$2T$: $g(\varepsilon)=1.25, 1.4$ for red and brown curves, respectively] and [$2C$: $g(\varepsilon)=1.25, 1.4$ for black and blue curves, respectively]. Right: $\alpha=1$ [$5T$: $g(\varepsilon)=1.3, 1.4$ for red and brown curves, respectively] and [$0.5C$: $g(\varepsilon)=1.3, 1.4$ for black and blue curves, respectively].

gravity one can show that the black hole temperature is not affected by the first order corrections [18]. Therefore, the black hole temperature, up to the leading order corrections, is just the same as that given by Eq. (3.1). By considering the leading order corrections, the black hole entropy gets logarithmic correction which can be written as [18,43,45]

$$S^{(TF)} = S - \frac{\xi}{2}\ln\left(ST^2\right), \tag{4.1}$$

where, S is the uncorrected black hole entropy given in Eq. (3.5), T being the black hole temperature (Eq. (3.1)) and ξ is the parameter of thermal fluctuations or correction parameter.

Now, making use of the corrected entropy (4.1) and temperature (3.1), one is able to calculate the Helmholtz free energy [18]. It can be obtained as

$$F^{(TF)} = -\int S^{(TF)}\,dT = \begin{cases} \frac{g(\varepsilon)}{4\pi b^2 f(\varepsilon)}\int S^{(TF)}\left(1+\Upsilon\right)\left(\frac{b}{r_+}\right)^{2(1-\alpha\gamma)}dr_+, \\ \quad \alpha\neq 1,\ \sqrt{3},\ \ (a) \\ \frac{g(\varepsilon)}{4\pi b^2 f(\varepsilon)}\int S^{(TF)}\left(1-\Upsilon_3\right)\left(\frac{b}{r_+}\right)^{1/2}dr_+, \\ \quad \alpha=\sqrt{3},\ \ (b) \\ \frac{g(\varepsilon)}{2\pi b f(\varepsilon)}\int S^{(TF)}\frac{dr_+}{r_+}, \qquad \alpha=1.\ \ (c) \end{cases} \tag{4.2}$$

By use of the obtained Helmholtz free energy, the black hole mass $M^{(TF)} = F^{(TF)} + TS^{(TF)}$, is obtained as

$$M^{(TF)} = F^{(TF)} + ST - \frac{T\xi}{2}\ln\left(ST^2\right), \tag{4.3}$$

where, $F^{(TF)}$ is given by Eq. (4.2), S and T are the uncorrected entropy and temperature, respectively.

As a matter of calculation it is easily shown that, although some of the thermodynamic quantities are affected by the thermal fluctuations, the first law of black hole thermodynamics is valid in the following form

$$dM^{(TF)} = T\,dS^{(TF)}. \tag{4.4}$$

In order to investigate the effects of thermal fluctuations on the stability of the black holes, starting from the relation $C^{(TF)} = T\frac{\partial S^{(TF)}}{\partial T}$, we obtained

$$C^{(TF)} = \begin{cases} \frac{2\pi b(\Upsilon-1)}{g^2(\varepsilon)(1-\alpha^2)(\Upsilon+1)}\left(\frac{b}{r_+}\right)^{2\alpha\gamma} \\ \quad -\xi\left[1+\frac{\Upsilon-1}{(1-\alpha^2)(\Upsilon+1)}\right], \qquad \alpha\neq 1,\ \sqrt{3},\ \ (a) \\ \frac{\pi b^2(1+\Upsilon_3)}{g^2(\varepsilon)(1-\Upsilon_3)}\left(\frac{r_+}{b}\right)^{\frac{1}{2}} \\ \quad -\frac{\xi}{2}\left(2+\frac{1+\Upsilon_3}{1-\Upsilon_3}\right), \qquad \alpha=\sqrt{3},\ \ (b) \\ -\frac{b\Lambda r_+}{g^2(\varepsilon)}\left[1-\frac{\Lambda b^2}{g^2(\varepsilon)}+\ln\left(\frac{b}{r_+}\right)\right] \\ \quad -\frac{\xi}{2}\left\{2+\left[1-\frac{\Lambda b^2}{g^2(\varepsilon)}+\ln\left(\frac{b}{r_+}\right)\right]\right\}, \quad \alpha=1.\ \ (c) \end{cases} \tag{4.5}$$

Eq. (4.5) indicates the heat capacity of dilaton black holes in which the quantum fluctuations are taken into account through consideration of the thermal fluctuations.

In order to examine the impacts of thermal fluctuations on the type-1 and type-2 phase transitions or stability of the new dilaton black holes, we have shown the plots of $C^{(TF)}$ in Figs. 6–8, for the cases $\alpha\neq 1$, $\sqrt{3}$, $\alpha=\sqrt{3}$ and $\alpha=1$, respectively. Fig. 6 shows that even if the black hole temperature is positive there is a point of type-1 phase transition we label by $r_+=r_2$. Also, the point $r_+=r_1$ is a point of type-2 phase transition. These are due to the thermal fluctuation consideration. This kind of dilaton black holes are stable for $r_+<r_1$ and $r_+>r_2$. As it is shown in Figs. 7 and 8, similar to the previous (uncorrected) case, no type-2 phase transition takes place and the physical black holes are unstable. There is a point of type-1 phase transition which in contrary to the uncorrected cases no longer coincides with the zero points of the black hole temperature.

5. Concluding remarks

The physical and thermodynamical properties of dilaton black holes have been investigated in an energy dependent space time with and without thermal fluctuations. The coupled equations of scalar and gravitational fields have been solved in the presence

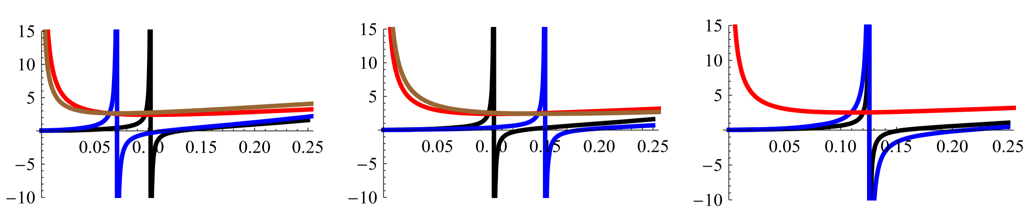

Fig. 6. T and $C^{(TF)}$ versus r_+ for $\Lambda=-3$, $f(\varepsilon)=0.5$ and $b=2.5$, Eqs. (3.1-a) and (4.5-a). Left: $g(\varepsilon)=0.25$, $\xi=2$ [$4\,T:\ \alpha=0.25, 0.35,$ for red and brown curves, respectively] and [$0.2C^{(TF)}:\ \alpha=0.25, 0.35,$ for black and blue curves, respectively]. Middle: $\alpha=0.25$, $\xi=2$ [$4\,T:\ g(\varepsilon)=0.25, 0.35,$ for red and brown curves, respectively] and [$0.2C^{(TF)}:\ \alpha=0.25, 0.35,$ for black and blue curves, respectively]. Right: $\alpha=0.25$, $g(\varepsilon)=0.3$[$10\,T:\ \xi=2, 3,$ for red and brown curves, respectively] and [$0.2C^{(TF)}:\ \xi=2, 3,$ for black and blue curves, respectively].

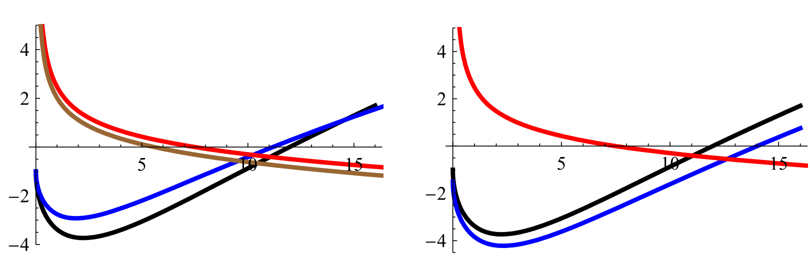

Fig. 7. T and $C^{(TF)}$ versus r_+ for $\Lambda=-3$, $f(\varepsilon)=0.75$ and $b=1.25$, Eqs. (3.1-b) and (4.5-b). Left: $\xi=2$, [$2\,T:\ g(\varepsilon)=1.25, 1.45,$ for red and brown curves, respectively] and [$C^{(TF)}:\ g(\varepsilon)=1.25, 1.45,$ for black and blue curves, respectively]. Right: $g(\varepsilon)=1.25$ [$2\,T:$ red curve] and [$C^{(TF)}:\ \xi=2, 3,$ for black and blue curves, respectively].

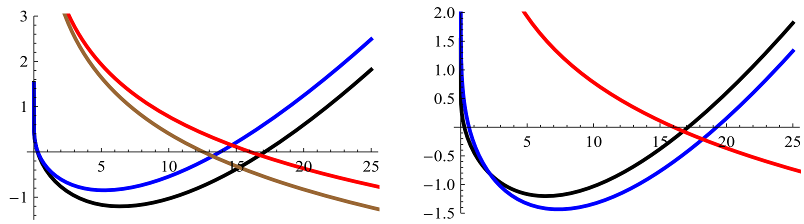

Fig. 8. T and $C^{(TF)}$ versus r_+ for $\Lambda = -3$, $f(\varepsilon) = 0.5$ and $b = 1$, Eqs. (3.1-c) and (4.5-c). Left: $\xi = 2$, [$4\,T$: $g(\varepsilon) = 1.3, 1.4$, for red and brown curves, respectively] and [$0.1C^{(TF)}$: $g(\varepsilon) = 1.3, 1.4$, for black and blue curves, respectively]. Right: $g(\varepsilon) = 1.3$, [$4\,T$: red curve] and [$0.1C^{(TF)}$: $\xi = 2, 6$ for black and blue curves, respectively].

of rainbow functions. We found that the dilaton potential can be written as a form of the linear combination of two Liouville-type potentials. According to alternative choices of dilaton parameters three different classes of dilaton black hole solutions have been introduced in gravity's rainbow. Through physical and mathematical interpretation of the solutions we found that: i) For the suitably fixed dilaton parameters, two horizon, extreme and naked singularity black holes can occur (Figs. 1–3). ii) The Ricci scalar of the solutions contains an essential singularity located at $r = 0$. iii) Due to the presence of dilaton scalar field, the asymptotic behavior of the solutions is neither flat nor A(dS). Existence of the horizons, as the real roots of the metric functions, and appearance of the singularities in the Ricci scalars are sufficient for the solutions to be considered as black holes.

The entropy and temperature associated to the horizon and the conserved mass of the black holes have been calculated. It has been shown that the temperature of the black holes with $\alpha \neq 1, \sqrt{3}$ can be positive valued for the properly fixed parameters (see Fig. 4). In the cases $\alpha = \sqrt{3}$ and $\alpha = 1$ the extreme black holes may occur at the points $r_+ = r_{3ext}$ and $r_+ = r_{1ext}$, respectively. Also, the physical and un-physical black holes can occur if the radiuses of their horizons are less or greater than those of extreme black holes, respectively (see Fig. 5). We obtained a Smarr-type formula for the mass as a function of the black hole entropy. We showed that the thermodynamic quantities satisfy the first law of black hole thermodynamics. It means that, even if some of the thermodynamic quantities are affected by the rainbow functions, the thermodynamical first law is still valid for either of the solutions obtained here. Next, making use of the canonical ensemble method and regarding the black hole heat capacity, we analyzed the black hole remnant or phase transitions for either of our new dilaton black holes. As it is shown in Fig. 4, for the black holes corresponding to $\alpha \neq 1, \sqrt{3}$, there is no point of type-1 phase transition. There is only one point of type-2 phase transition at the point $r_+ = r_0$, where the black hole heat capacity diverges. These black holes are stable for $r_+ > r_0$. The black holes with $\alpha = \sqrt{3}$ and $\alpha = 1$ undergo type-1 phase transition located at $r_+ = r_{3ext}$ and $r_+ = r_{1ext}$, respectively. Note that the points of type-1 phase transition are exactly the vanishing points of the temperatures. No type-2 phase transition takes place for these kinds of black holes and the physical black holes are unstable (see Fig. 5).

At the final stage, by considering the black hole thermal fluctuations, we calculated the corrected thermodynamic quantities. Although, some of them contain correction terms when the thermal fluctuations are taken into account, the first law of black hole thermodynamics remains valid. We found that, in the presence of black hole fluctuations, the black hole heat capacity receives some corrections. As the results: a) In the case $\alpha \neq 1, \sqrt{3}$, with the positive valued temperature, there is again one point of type-2 phase transition located at $r_+ = r_1$ but, in spite of the uncorrected case, there is a point of type-1 phase transition at the point $r_+ = r_2$. The black holes with $r_+ < r_1$ and $r_+ > r_2$ are locally stable. b) The black holes corresponding to $\alpha = \sqrt{3}$ and $\alpha = 1$ cases, just like the uncorrected case do not undergo type-2 phase transition and show only one point of type-1 phase transition. But this time, in spite of the uncorrected case, the points of type-1 phase transition no longer coincide with the vanishing points of the black hole temperatures (see Figs. 6–8).

Acknowledgement

The author thanks the Razi University Research Council for official supports of this work.

References

[1] J. Alfaro, H.A. Morales-Técotl, L.F. Urrutia, Phys. Rev. Lett. 84 (2000) 2318.
[2] G. Amelino-Camelia, M. Arzano, A. Procaccini, Phys. Rev. D 70 (2004) 107501.
[3] G. Amelino-Camelia, M. Arzano, Y. Ling, G. Mandanici, Class. Quantum Gravity 23 (2006) 2585.
[4] G. Amelino-Camelia, M. Arzano, A. Procaccini, Int. J. Mod. Phys. D 13 (2004) 2337.
[5] G. Amelino-Camelia, Nature 410 (2001) 1065.
[6] G. Amelino-Camelia, Int. J. Mod. Phys. D 11 (2002) 35.
[7] R. Garattini, E.N. Saridakis, Int. J. Mod. Phys. D 25 (2016) 1650101.
[8] A.F. Ali, Phys. Rev. D 89 (2014) 104040.
[9] G. Amelino-Camelia, Phys. Lett. B 510 (2001) 255.
[10] G. Amelino-Camelia, Int. J. Mod. Phys. D 11 (2002) 35.
[11] J. Magueijo, L. Smolin, Phys. Rev. Lett. 88 (2002) 190403.
[12] V.A. Kostelecky, S. Samuel, Phys. Rev. D 39 (1989) 683.
[13] J. Magueijo, L. Smolin, Class. Quantum Gravity 21 (2004) 1725.
[14] A.F. Ali, Phys. Rev. D 89 (2014) 104040.
[15] P. Horava, Phys. Rev. D 79 (2009) 084008.
[16] P. Horava, Phys. Rev. Lett. 102 (2009) 161301.
[17] S.H. Hendi, Gen. Relativ. Gravit. 48 (2016) 50.
[18] S.H. Hendi, B. Eslam Panah, S. Panahiyan, M. Momennia, Eur. Phys. J. C 77 (2017) 647.
[19] S.H. Hendi, M. Faizal, B. Eslam Panah, S. Panahiyan, M. Momennia, Eur. Phys. J. C 76 (2016) 296.
[20] S.H. Hendi, S. Panahiyan, B. Eslam Panah, M. Momennia, Eur. Phys. J. C 76 (2016) 150.
[21] Y. Ling, X. Li, H. Zhang, Phys. Lett. A 22 (2007) 2749.
[22] M. Dehghani, Phys. Lett. B 777 (2018) 351.
[23] S.H. Hendi, M. Faizal, Phys. Rev. D 92 (2015) 044027.
[24] Z-W. Feng, S-Z. Yang, Phys. Lett. B 772 (2017) 737.
[25] J. Magueijo, L. Smolin, Phys. Rev. D 67 (2003) 044017.
[26] G. Amelino-Camelia, Living Rev. Relativ. 16 (2013) 5.
[27] G. Amelino-Camelia, J.r. Ellis, N. Mavromatos, D.V. Nanopoulos, Int. J. Mod. Phys. A 12 (1997) 607.
[28] G. Amelino-Camelia, J.R. Ellis, N.E. Mavromatos, D.V. Nanopoulos, S. Sarkar, Nature 393 (1998) 763.
[29] A.F. Ali, M. Faizal, M.M. Khalile, Nucl. Phys. B 894 (2015) 341.
[30] A.F. Ali, Phys. Rev. D 89 (2014) 104040.
[31] S.H. Hendi, M. Momennia, B. Eslam Panah, M. Faizal, Astrophys. J. 827 (2016) 153.
[32] S.W. Hawking, Nature 248 (1974) 30.
[33] S.W. Hawking, Commun. Math. Phys. 43 (1975) 199.
[34] S.W. Hawking, Phys. Rev. D 72 (2005) 084013.
[35] J.D. Bekenstein, Phys. Rev. D 7 (1973) 2333.
[36] J.M. Bardeen, B. Carter, S.W. Hawking, Commun. Math. Phys. 31 (1973) 161.
[37] S.H. Hendi, B. Eslam Panah, S. Panahiyan, M. Momennia, Adv. High Energy Phys. 2016 (2016) 9813582.
[38] S.H. Hendi, R.B. Mann, N. Riazi, B. Eslam Panah, Phys. Rev. D 86 (2012) 104034.
[39] M. Dehghani, S.F. Hamidi, Phys. Rev. D 96 (2017) 044025.
[40] M. Dehghani, Phys. Rev. D 96 (2017) 044014.
[41] M. Dehghani, Phys. Lett. B 773 (2017) 105.
[42] S.H. Hendi, B. Eslam Panah, R. Saffari, Int. J. Mod. Phys. D 23 (2014) 1550088.

[43] B. Pourhassan, M. Faizal, S. Upadhyay, L. Al Asfar, Eur. Phys. J. C 77 (2017) 555.
[44] S. Upadhyay, B. Pourhassan, H. Farahani, Phys. Rev. D 95 (2017) 106014.
[45] S. Upadhyay, Phys. Lett. B 775 (2017) 130.
[46] M. Dehghani, Phys. Lett. B 749 (2015) 125.
[47] B. Pourhassan, M. Faizal, Z. Zaz, A. Bhat, Phys. Lett. B 773 (2017) 325.
[48] B. Pourhassan, M. Faizal, S. Capozziello, Ann. Phys. 377 (2017) 108.
[49] B. Pourhassan, M. Faizal, Europhys. Lett. 111 (2015) 40006.
[50] M. Faizal, B. Pourhassan, Phys. Lett. B 751 (2015) 487.
[51] B. Pourhassan, M. Faizal, Phys. Lett. B 755 (2016) 444.
[52] B. Pourhassan, M. Faizal, U. Debnath, Eur. Phys. J. C 77 (2016) 145.
[53] B. Pourhassan, M. Faizal, Nucl. Phys. B 913 (2016) 834.
[54] S.H. Hendi, B. Eslam Panah, S. Panahiyan, A. Sheykhi, Phys. Lett. B 767 (2017) 214.
[55] M. Dehghani, Int. J. Mod. Phys. D 27 (2018) 1850073.
[56] M. Dehghani, Phys. Rev. D 97 (2018) 044030.
[57] S.H. Hendi, S. Panahiyan, M. Momennia, Int. J. Mod. Phys. D 25 (2016) 1650063.
[58] S.H. Hendi, S. Panahiyan, B. Eslampanah, Eur. Phys. J. C 75 (2015) 296.
[59] M. Dehghani, Phys. Rev. D 94 (2016) 104071.
[60] M. Dehghani, S.F. Hamidi, Phys. Rev. D 96 (2017) 104017.